

Remote Sensing Data Collection LiDAR and Digital Orthophotos

Cottonwood Canyon, OR

July 23, 2010

Submitted to:

Brady Callahan
Oregon Parks & Recreation
725 Summer St. NE, Ste C
Salem, OR 97301

Submitted by:

Watershed Sciences
517 SW 2nd Street, Suite 400
Corvallis, OR 97333

529 SW 3rd Ave. Suite 300
Portland, Oregon 97204

www.watershedsciences.com

LiDAR Remote Sensing Data Collection: Cottonwood Canyon, OR

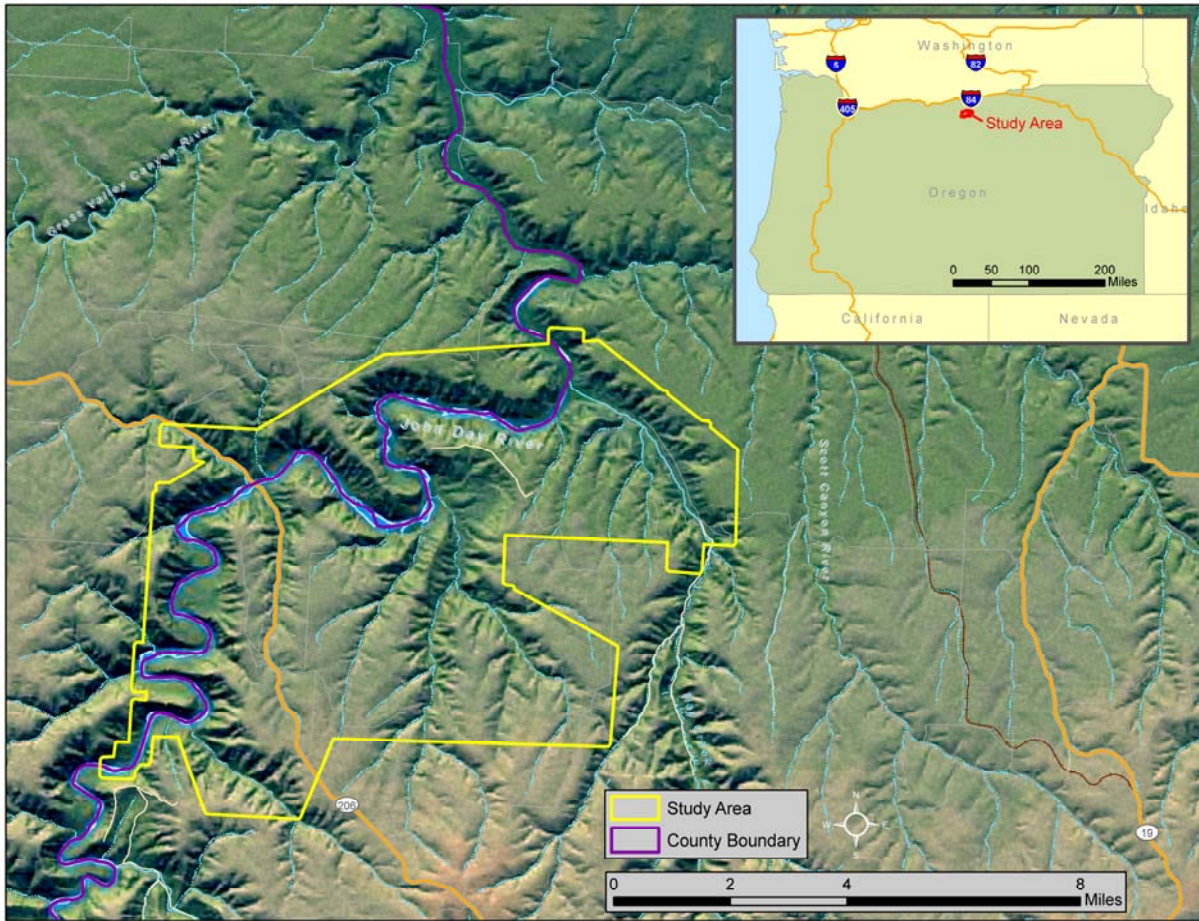
TABLE OF CONTENTS

1. Overview	4
2. Acquisition	5
2.1 Airborne Survey - Instrumentation and Methods	5
2.2 Mapping Control and Check Points - Instrumentation and Methods.....	6
2.2.1 Mapping Control.....	6
2.2.2 RTK Survey	7
3.1 Applications and Work Flow Overview	5
3.2 Aircraft Kinematic GPS and IMU Data	6
3.3 Laser Point Processing.....	6
3.4 Orthophotograph Processing	7
4. LiDAR Accuracy Assessment	7
4.1 Laser Noise and Relative Accuracy	7
4.2 Absolute Accuracy	8
5. Photo Accuracy Assessment	9
6. Study Area Results.....	10
6.1 Data Summary	10
*See section 6.2 for explanation	10
6.2 Data Density/Resolution	10
6.3 Relative Accuracy Calibration Results	13
6.4 Absolute Accuracy	14
6.5 Orthophotograph Accuracy	15
7. Projection/Datum and Units	17
8. Deliverables	17
9. Selected Images	18
10. Glossary.....	22
11. Citations	23
Appendix B	25

1. Overview

Watershed Sciences, Inc. (WS) collected Light Detection and Ranging (LiDAR) data and natural-color orthophotographs of Cottonwood Canyon from May 13th to 15th, 2010. The study area is located in Gilliam and Sherman County, Oregon. The total area of this delivery of LiDAR and true color orthophotographs is 35,902 acres including a 100 m buffer (Figure 1).

Figure 1. Cottonwood Canyon study area.



2. Acquisition

2.1 Airborne Survey - Instrumentation and Methods

The LiDAR survey used a Leica ALS50 Phase II laser system. For the Cottonwood Canyon study area the sensor scan angle was $\pm 14^\circ$ from nadir¹ with a pulse rate designed to yield an average native density (number of pulses emitted by the laser system) of ≥ 8 points per square meter over terrestrial surfaces. It is not uncommon for some types of surfaces (e.g. dense vegetation or water) to return fewer pulses than the laser originally emitted. These discrepancies between ‘native’ and ‘delivered’ density will vary depending on terrain, land cover and the prevalence of water bodies.

All survey areas were surveyed with an opposing flight line side-lap of $\geq 50\%$ (=100% overlap) to reduce laser shadowing and increase surface laser painting. The Leica ALS50 Phase II system allows up to four range measurements (returns) per pulse, and all discernable laser returns were processed for the output dataset.

The aerial imagery was collected using a Leica RCD-105 medium format digital camera. For the Cottonwood Canyon study area, images were collected in 3 spectral bands (red, green, blue) with 60% along track overlap and 40% sidelap between frames. The acquisition flight parameters were designed to yield native pixel resolution of 10-31cm.



The Cessna Caravan is a stable platform, ideal for flying slow and low for high density projects. The Leica ALS50 sensor head installed in the Caravan is shown on the left.

To accurately solve for laser point position (geographic coordinates x, y, z), the positional coordinates of the airborne sensor and the attitude of the aircraft were recorded continuously throughout the LiDAR data collection mission. Aircraft position was measured twice per second (2 Hz) by an onboard differential GPS unit. Aircraft attitude was measured 200 times per second (200 Hz) as pitch, roll and yaw (heading) from an onboard inertial measurement unit (IMU). To allow for post-processing correction and calibration, aircraft/sensor position and attitude data are indexed by GPS time.

¹ Nadir refers to the perpendicular vector to the ground directly below the aircraft. Nadir is commonly used to measure the angle from the vector and is referred to a “degrees from nadir”.

2.2 Mapping Control and Check Points - Instrumentation and Methods

The following ground survey data were collected to enable the geo-spatial correction of the aircraft positional coordinate data collected throughout the flight, and to allow for quality assurance checks on final LiDAR data products.

2.2.1 Mapping Control

The mapping control plan was designed to provide redundant controls within 13 nautical miles of the mission area for LiDAR flights. The controls were set prior to the airborne missions with control coordinates established using GPS receivers and multiple, long occupations. Dr. Michael Wing, OR PLS #65717, provided survey oversight and certification of the project controls. The mapping control certification report is contained in **Appendix B**.

Simultaneous with the airborne data collection mission, we conducted multiple static (1 Hz recording frequency) ground surveys over the control monuments (**Table 1**). Indexed by time, these GPS data are used to correct the continuous onboard measurements of aircraft position recorded throughout the mission. The control coordinates for each GPS occupation were checked for consistency and to confirm antenna heights.



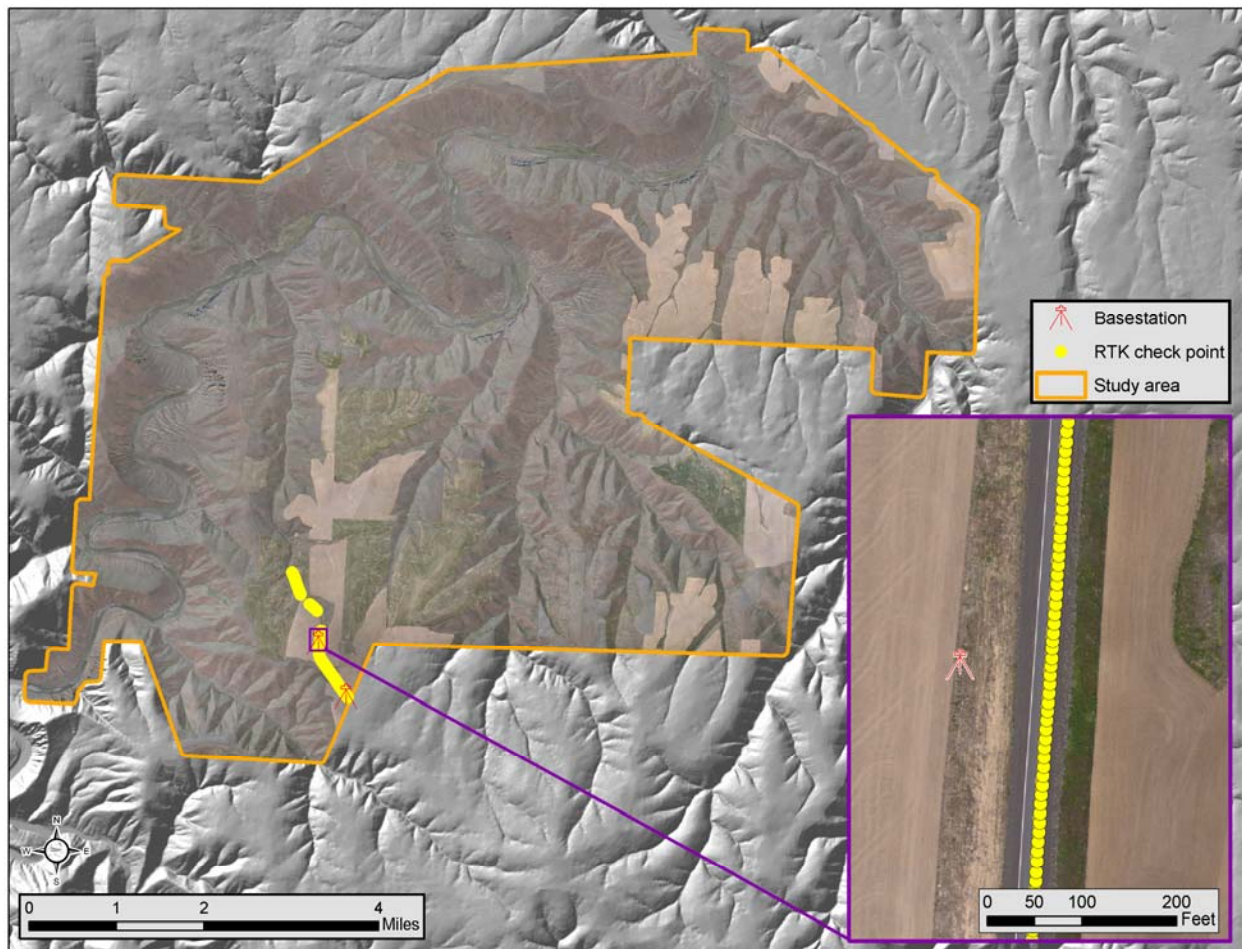
Table 1. Base Station Control coordinates for the Cottonwood Canyon study area.

Base Station ID	Datum: NAD83 (CORS96)		GRS80
	Latitude	Longitude	Ellipsoid Z (meters)
CC_AW1	45° 24' 19.79846"	120° 26' 38.35690"	623.000
CC_AW2	45° 24' 51.35794"	120° 27' 03.73336"	599.202

2.2.2 RTK Check Points

To assess LiDAR data accuracy, ground truth points were collected using GPS based real-time kinematic (RTK) survey techniques. For an RTK survey, the ground crew uses a roving unit to receive radio-relayed corrected positional coordinates for all ground points from a GPS base station set up over a survey control monument. Instrumentation includes multiple Trimble DGPS units (R8). RTK surveying allows for precise location measurements with an error (σ) of ≤ 1.5 cm. **Figure 2** below portrays a distribution of base station and RTK point locations used for the survey areas.

Figure 2. RTK and base station locations used for the Cottonwood Canyon study area.



3. Data Processing

3.1 Applications and Work Flow Overview

1. Resolved kinematic corrections for aircraft position data using kinematic aircraft GPS and static ground GPS data with certified mapping control.
Software: Waypoint GPS v.8.10, Trimble Geomatics Office v.1.62
2. Developed a smoothed best estimate of trajectory (SBET) file that blends post-processed aircraft position with attitude data. Sensor head position and attitude were calculated throughout the survey. The SBET data were used extensively for laser point processing.
Software: IPAS v.1.35
3. Calculated laser point position by associating SBET position to each laser point return time, scan angle, intensity, etc. Created raw laser point cloud data for the entire survey in *.las (ASPRS v. 1.2) format.
Software: ALS Post Processing Software v.2.7
4. Imported raw laser points into manageable blocks (less than 500 MB) to perform manual relative accuracy calibration and filter for pits/birds. Ground points were then classified for individual flight lines (to be used for relative accuracy testing and calibration).
Software: TerraScan v.10.009
5. Using ground classified points per each flight line, the relative accuracy was tested. Automated line-to-line calibrations were then performed for system attitude parameters (pitch, roll, heading), mirror flex (scale) and GPS/IMU drift. Calibrations were performed on ground classified points from paired flight lines. Every flight line was used for relative accuracy calibration.
Software: TerraMatch v.10.006
6. Position and attitude data were imported. Resulting data were classified as ground and non-ground points. Statistical absolute accuracy was assessed via direct comparisons of ground classified points to ground RTK survey data. Data were then converted to orthometric elevations (NAVD88) by applying a Geoid03 correction. Ground models were created as a triangulated surface and exported as ArcInfo ASCII grids at a 1-meter pixel resolution.
Software: TerraScan v.10.009, ArcMap v. 9.3.1, TerraModeler v.10.004
7. Converted raw images to tif format, calibrating raw image pixels for gain and exposure settings of each image.
Software: Leica Calibration Post Processing v.1.0.4
8. Calculated photo position and orientation by associating the SBET position (Step 3) to each image capture time.
Software: IPASCO v.1.3
9. Orthorectified calibrated tiffs utilizing photo orientation information (Step 8) and the LiDAR-derived ground surface (Step 6).
Software: Leica Photogrammetry Suite v.9.2
10. To correct light imbalances between overlapping images, radiometric global tilting adjustments were applied to the rectified images.
Software: OrthoVista v.4.4.
11. The color corrected images were then mosaicked together for the survey area and subset into tiles to make the file size more manageable.
Software: OrthoVista v.4.4.
12. Mosaicked tiles were inspected for misalignments introduced by automatic seam generation. Misalignments were corrected by manual adjustments to seams.
Software: Adobe Photoshop 7.0, OrthoVista v.4.4.

3.2 Aircraft Kinematic GPS and IMU Data

LiDAR survey datasets were referenced to the 1 Hz static ground GPS data collected over pre-surveyed monuments with known coordinates. While surveying, the aircraft collected 2 Hz kinematic GPS data, and the onboard inertial measurement unit (IMU) collected 200 Hz aircraft attitude data. Leica IPAS Suite was used to process the kinematic corrections for the aircraft. The static and kinematic GPS data were then post-processed after the survey to obtain an accurate GPS solution and aircraft positions. Waypoint was used to develop a trajectory file that includes corrected aircraft position and attitude information. The trajectory data for the entire flight survey session were incorporated into a final smoothed best estimated trajectory (SBET) file that contains accurate and continuous aircraft positions and attitudes.

3.3 Laser Point Processing

Laser point coordinates were computed using the IPAS and ALS Post Processor software suites based on independent data from the LiDAR system (pulse time, scan angle), and aircraft trajectory data (SBET). Laser point returns (first through fourth) were assigned an associated (x, y, z) coordinate along with unique intensity values (0-255). The data were output into large LAS v. 1.2 files; each point maintains the corresponding scan angle, return number (echo), intensity, and x, y, z (easting, northing, and elevation) information.

These initial laser point files were too large for subsequent processing. To facilitate laser point processing, bins (polygons) were created to divide the dataset into manageable sizes (< 500 MB). Flightlines and LiDAR data were then reviewed to ensure complete coverage of the survey area and positional accuracy of the laser points.

Laser point data were imported into processing bins in TerraScan, and manual calibration was performed to assess the system offsets for pitch, roll, heading and scale (mirror flex). Using a geometric relationship developed by Watershed Sciences, Inc., each of these offsets was resolved and corrected if necessary.

LiDAR points were filtered for noise, pits (artificial low points) and birds (true birds as well as erroneously high points) by screening for absolute elevation limits, isolated points and height above ground. Each bin was then manually inspected for remaining pits and birds and spurious points were removed. In a bin containing approximately 7.5-9.0 million points, an average of 50-100 points are typically found to be artificially low or high. Common sources of non-terrestrial returns are clouds, birds, vapor, haze, decks, brush piles, etc.

Internal calibration was refined using TerraMatch. Points from overlapping lines were tested for internal consistency and final adjustments were made for system misalignments (i.e., pitch, roll, heading offsets and scale). Automated sensor attitude and scale corrections yielded 3-5 cm improvements in the relative accuracy. Once system misalignments were corrected, vertical GPS drift was then resolved and removed per flight line, yielding a slight improvement (<1 cm) in relative accuracy.

The TerraScan software suite is designed specifically for classifying near-ground points (Soininen, 2004). The processing sequence began by 'removing' all points that were not 'near' the earth based on geometric constraints used to evaluate multi-return points. The resulting bare earth (ground) model was visually inspected and additional ground point

modeling was performed in site-specific areas to improve ground detail. This manual editing of grounds often occurs in areas with known ground modeling deficiencies, such as: bedrock outcrops, cliffs, deeply incised stream banks, and dense vegetation. In some cases, automated ground point classification erroneously included known vegetation (i.e., understory, low/dense shrubs, etc.). These points were manually reclassified as non-grounds. Ground surface rasters were developed from triangulated irregular networks (TINs) of ground points.

3.4 Orthophotograph Processing

Image radiometric values were calibrated to specific gain and exposure settings associated with each capture using Leica's Calibration Post Processing software. The calibrated images were saved in tiff format to be used as inputs for the rectification process. Photo position and orientation was then calculated by assigning aircraft position and attitude information to each image by associating the time of image capture with trajectory file (SBET) in IPASCO. Photos were then orthorectified to the LiDAR derived ground surface using LPS. This typically results in <2 pixel relative accuracy between images. Relative accuracy can vary slightly with terrain but offsets greater than 2 pixels tend to manifest at the image edges which are typically removed in the mosaic process.

The rectified images were mosaicked together in a three step process using Orthovista. Firstly color correction was applied to each image using global tilting adjustments designed to homogenize overlapping regions. Secondly, discrepancies between images were minimized by an automated seam generation process. The most nadir portion of each image was selected and seams were drawn around landscape features. The high resolution orthophotos were delineated into 1/100th USGS quads appropriate to the pixel resolution and requested spatial reference.

4. LiDAR Accuracy Assessment

Our LiDAR quality assurance process uses the data from the real-time kinematic (RTK) ground survey conducted in the survey area. In this project, a total of **686** RTK GPS measurements were collected on hard surfaces distributed among multiple flight swaths. To assess absolute accuracy, we compared the location coordinates of these known RTK ground survey points to those calculated for the closest laser points.

4.1 Laser Noise and Relative Accuracy

Laser point absolute accuracy is largely a function of laser noise and relative accuracy. To minimize these contributions to absolute error, we first performed a number of noise filtering and calibration procedures prior to evaluating absolute accuracy.

Laser Noise

For any given target, laser noise is the breadth of the data cloud per laser return (i.e., last, first, etc.). Lower intensity surfaces (roads, rooftops, still/calm water) experience higher laser noise. The laser noise range for this survey was approximately 0.02 meters (0.07 ft).

Relative Accuracy

Relative accuracy refers to the internal consistency of the data set - the ability to place a laser point in the same location over multiple flight lines, GPS conditions, and aircraft attitudes. Affected by system attitude offsets, scale, and GPS/IMU drift, internal consistency is measured as the divergence between points from different flight lines within an overlapping area. Divergence is most apparent when flight lines are opposing. When the LiDAR system is well calibrated, the line-to-line divergence is low (<10 cm). See Appendix A for further information on sources of error and operational measures that can be taken to improve relative accuracy.

Relative Accuracy Calibration Methodology

1. Manual System Calibration: Calibration procedures for each mission require solving geometric relationships that relate measured swath-to-swath deviations to misalignments of system attitude parameters. Corrected scale, pitch, roll and heading offsets were calculated and applied to resolve misalignments. The raw divergence between lines was computed after the manual calibration was completed and reported for each survey area.
2. Automated Attitude Calibration: All data were tested and calibrated using TerraMatch automated sampling routines. Ground points were classified for each individual flight line and used for line-to-line testing. System misalignment offsets (pitch, roll and heading) and scale were solved for each individual mission and applied to respective mission datasets. The data from each mission were then blended when imported together to form the entire area of interest.
3. Automated Z Calibration: Ground points per line were utilized to calculate the vertical divergence between lines caused by vertical GPS drift. Automated Z calibration was the final step employed for relative accuracy calibration.

4.2 Absolute Accuracy

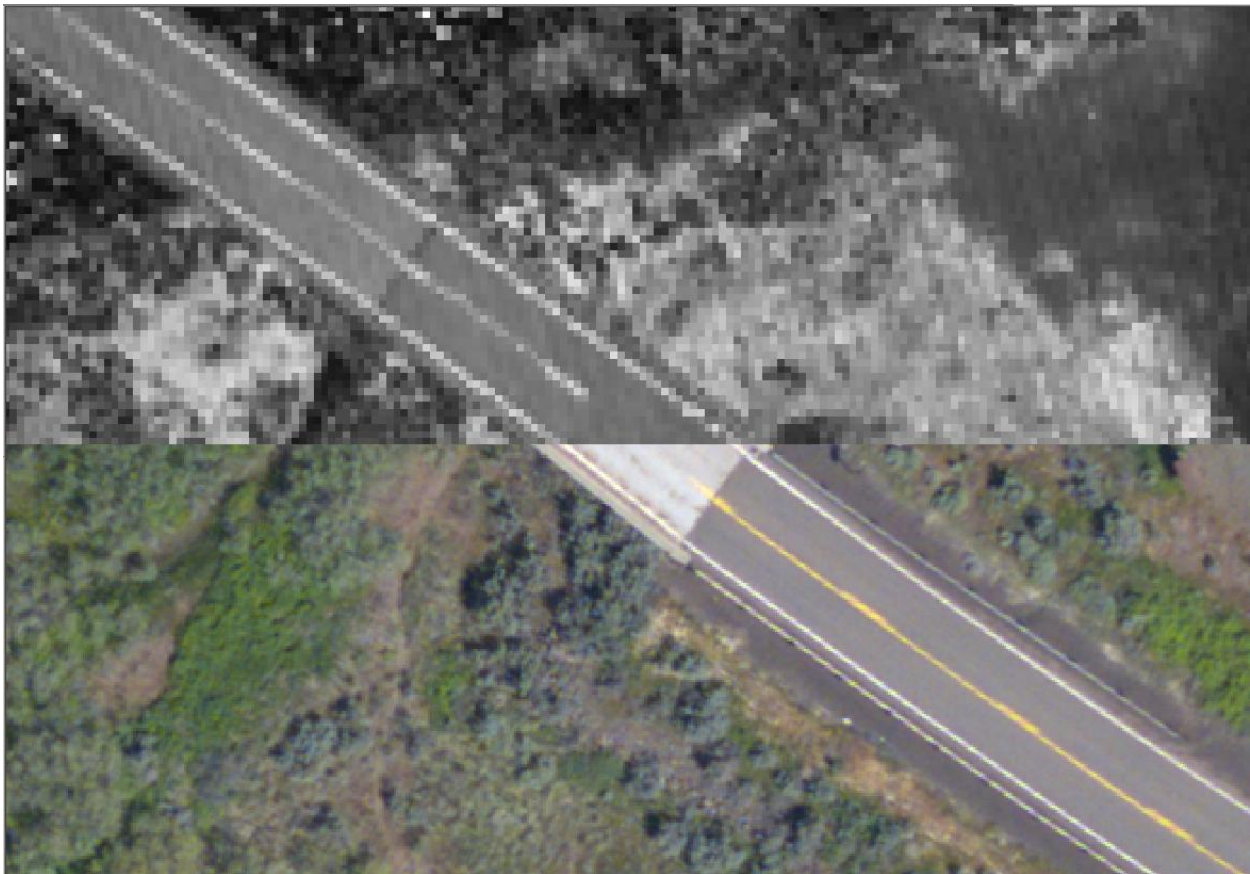
The vertical accuracy of the LiDAR data is described as the mean and standard deviation ($\sigma \sim \sigma$) of divergence of LiDAR point coordinates from RTK ground survey point coordinates. To provide a sense of the model predictive power of the dataset, the root mean square error (RMSE) for vertical accuracy is also provided. These statistics assume the error distributions for x, y, and z are normally distributed, thus we also consider the skew and kurtosis of distributions when evaluating error statistics.

Statements of statistical accuracy apply to fixed terrestrial surfaces only and may not be applied to areas of dense vegetation or steep terrain. To calibrate laser accuracy for the LiDAR dataset, 686 RTK ground survey points were collected on fixed, hard-packed road surfaces within the survey area.

5. Photo Accuracy Assessment

To assess spatial accuracy of the orthophotographs they are compared against check points identified from the LiDAR intensity images. The check points were collected and measured on surface features such as painted road-lines and corners of sidewalks. The accuracy of the final mosaic, expressed as root mean square error (RMSE), was calculated in relation to the LiDAR-derived check points. **Figure 3** displays the co-registration between orthorectified photographs and LiDAR intensity images.

Figure 3. Example of co-registration of color images with LiDAR intensity images.



6. Study Area Results

Summary statistics for point resolution and accuracy (relative and absolute) of the LiDAR data collected in the Cottonwood Canyon study area are presented below in terms of central tendency, variation around the mean, and the spatial distribution of the data (for point resolution by tile).

6.1 Data Summary

Table 2. Resolution and Accuracy - Specifications and Achieved Values.

	Targeted	Achieved
Resolution:	≥ 8 points/m ² (0.74 points/ft ²)	9.47 points/m ² (0.88 points/ft ²)
Vertical Accuracy (1 σ):	<15 cm (0.49 ft)	2.9 cm (1.1 in)

*See section 6.2 for explanation

6.2 Data Density/Resolution

Certain types of surfaces (e.g. water, dense vegetation, breaks in terrain, steep slopes) may return fewer pulses (delivered density) than the laser originally emitted (native density).

Ground classifications were derived from automated ground surface modeling and manual, supervised classifications where it was determined that the automated model had failed. Ground-classified return densities will be lower in areas of dense vegetation, water, or buildings. **Figures 6** displays the distribution of average first-return and ground-classified point densities by processing tile

Data Resolution for the Cottonwood Canyon study area:

- Average Point (First Return) Density = 9.47 points/m² (0.88 points/ft²)
- Average Ground Point Density = 3.03 points/m² (0.28 points/ft²)

Figure 4. Density distribution for first return laser points.

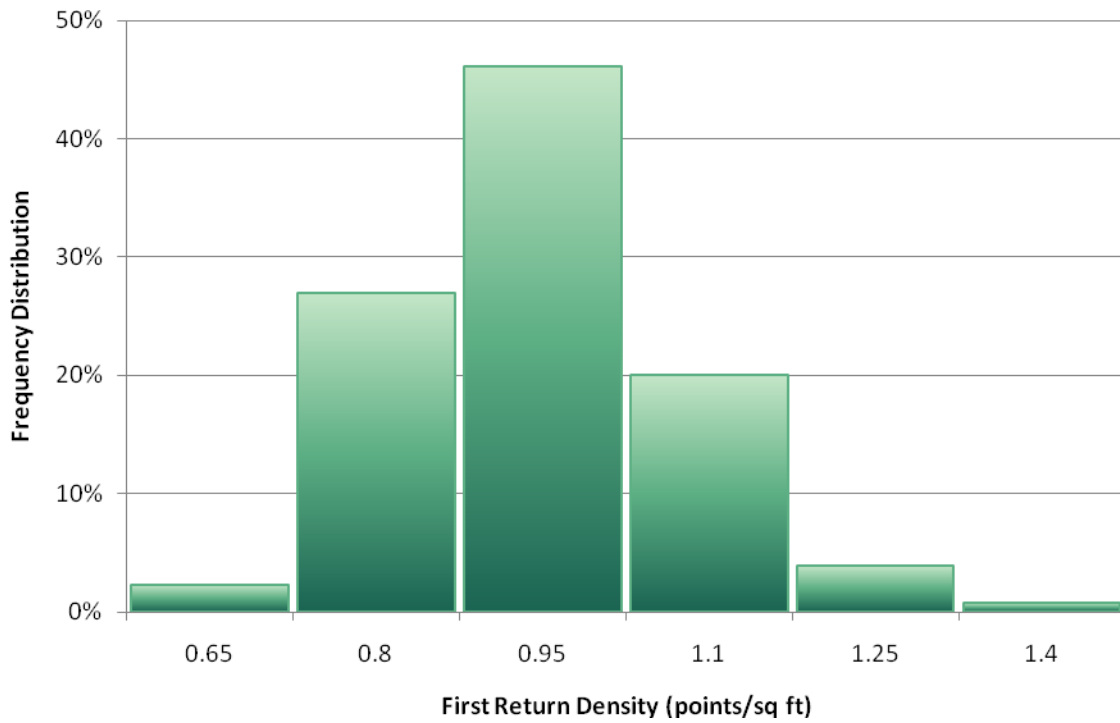


Figure 5. Density distribution for ground classified laser points.

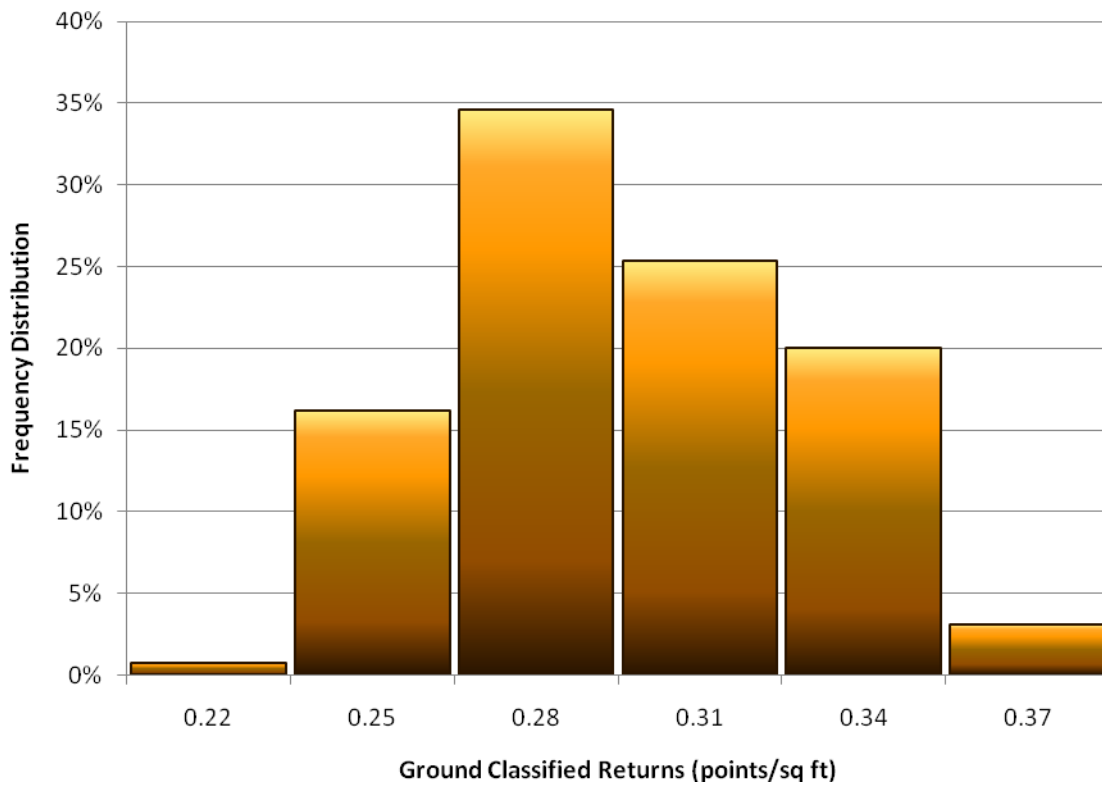
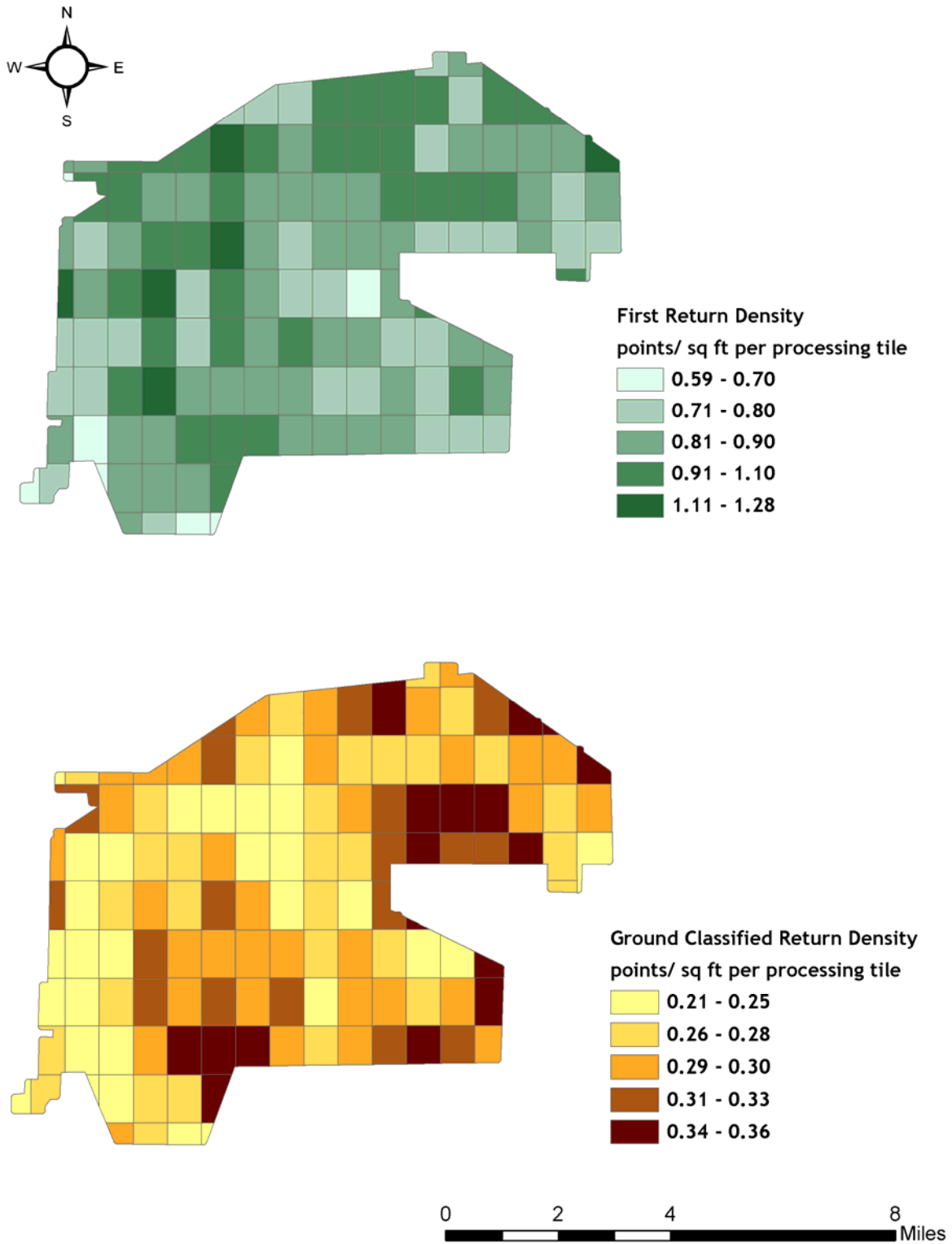


Figure 6. Ground classified and first return laser point data density per processing tile.

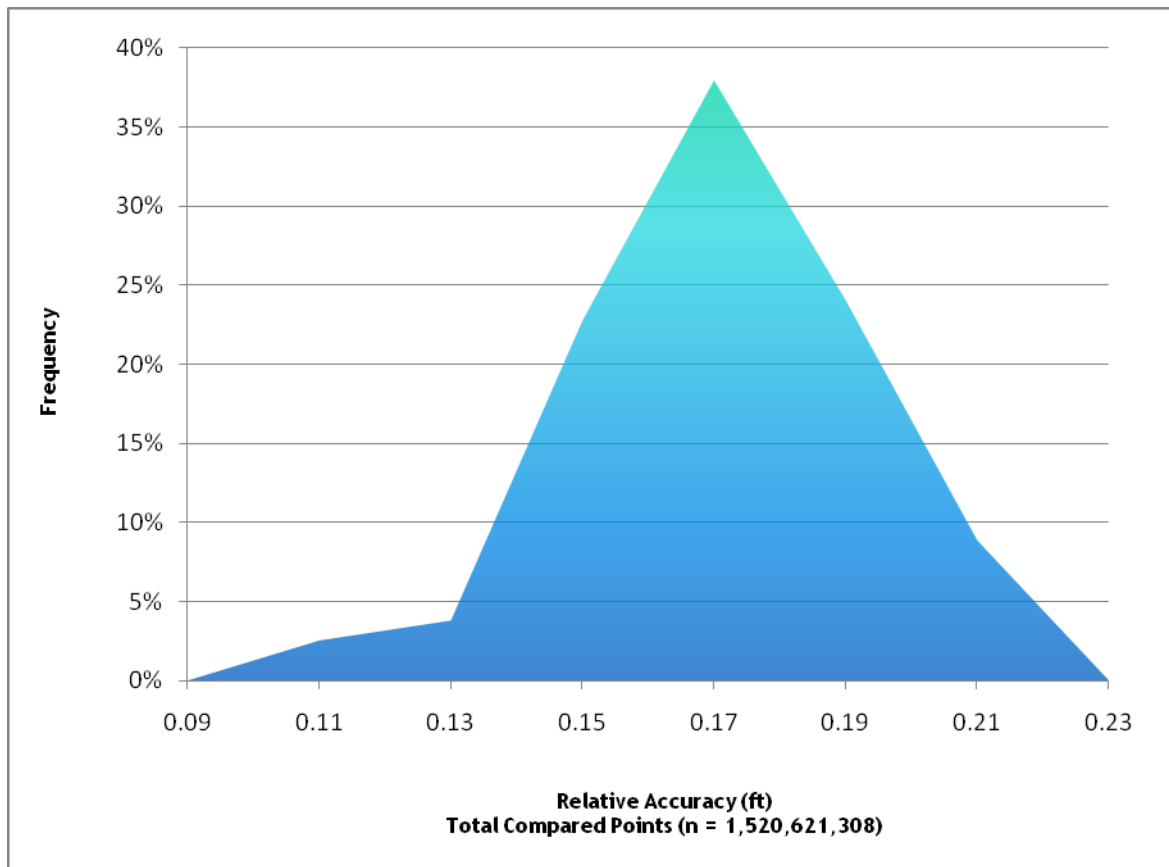


6.3 Relative Accuracy Calibration Results

Relative accuracies for the Cottonwood Canyon study area measure the full survey calibration including areas outside the delivered boundary:

- Project Average = 0.16 ft
- Median Relative Accuracy = 0.16 ft
- 1σ Relative Accuracy = 0.023 ft
- 2σ Relative Accuracy = 0.046 ft

Figure 7. Distribution of relative accuracies per flight line, non slope-adjusted



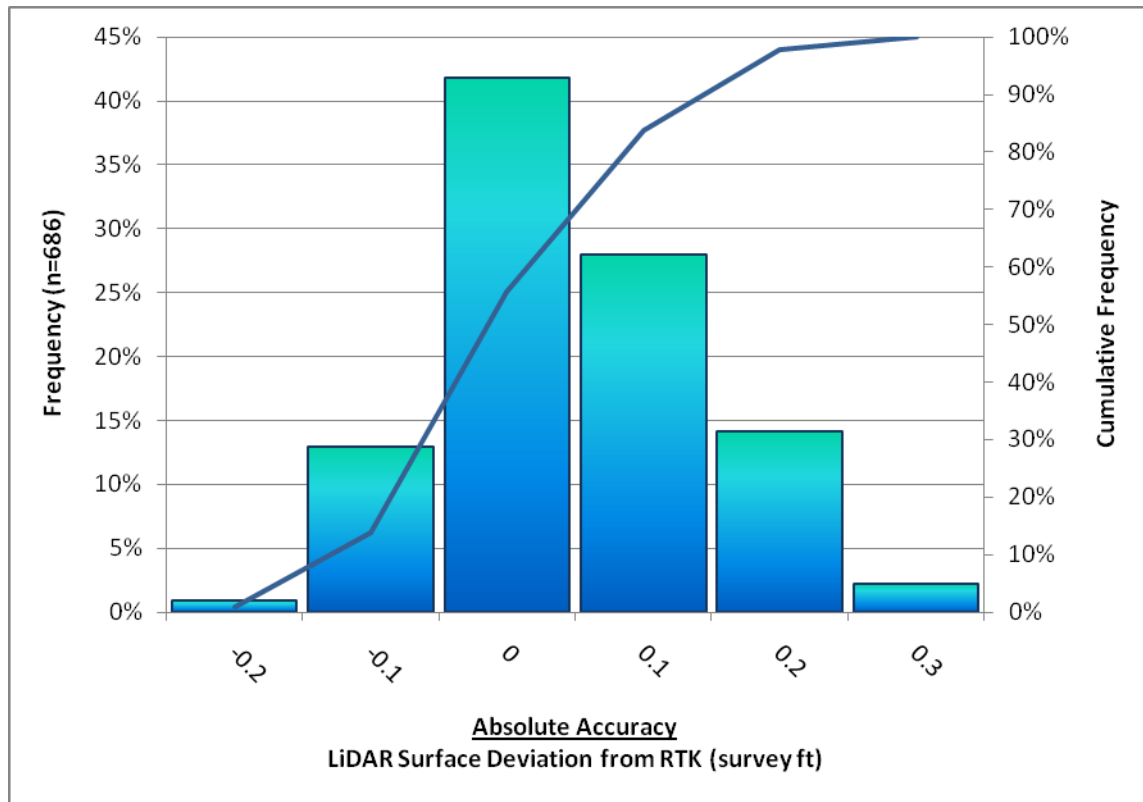
6.4 Absolute Accuracy

Absolute accuracies for the Cottonwood Canyon survey area:

Table 3. Absolute Accuracy - Deviation between laser points and RTK hard surface survey points (survey feet).

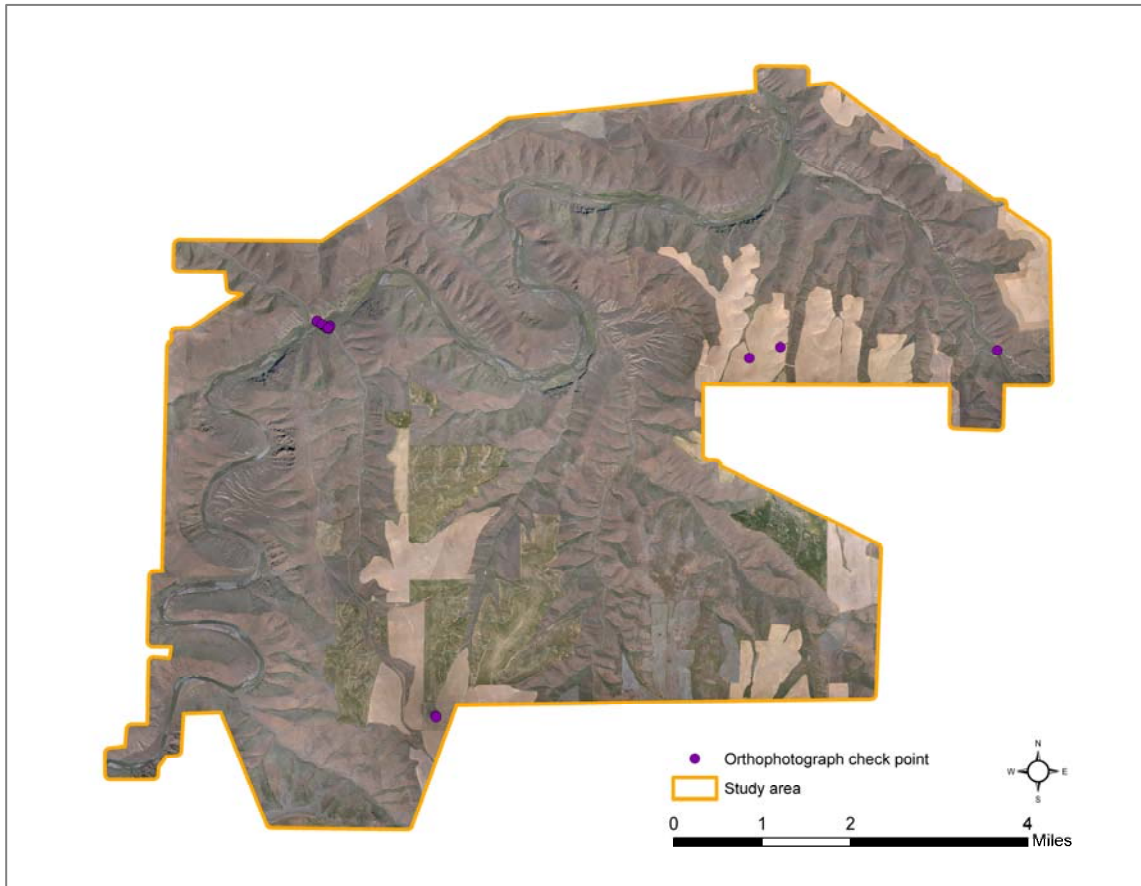
RTK Survey Sample Size (n): 686	
Root Mean Square Error (RMSE) = 0.094 ft	Minimum Δz = -0.28 ft
Standard Deviations:	Maximum Δz = 0.27 ft
1 sigma (σ) = 0.053 ft 2 sigma (σ) = 0.10 ft	Average Δz = -0.002 ft

Figure 8. Absolute Accuracy - Histogram Statistics, based on 686 hard surface points.



6.5 Orthophotograph Accuracy

Figure 9. Orthophotograph check point location map for Cottonwood Canyon study area.

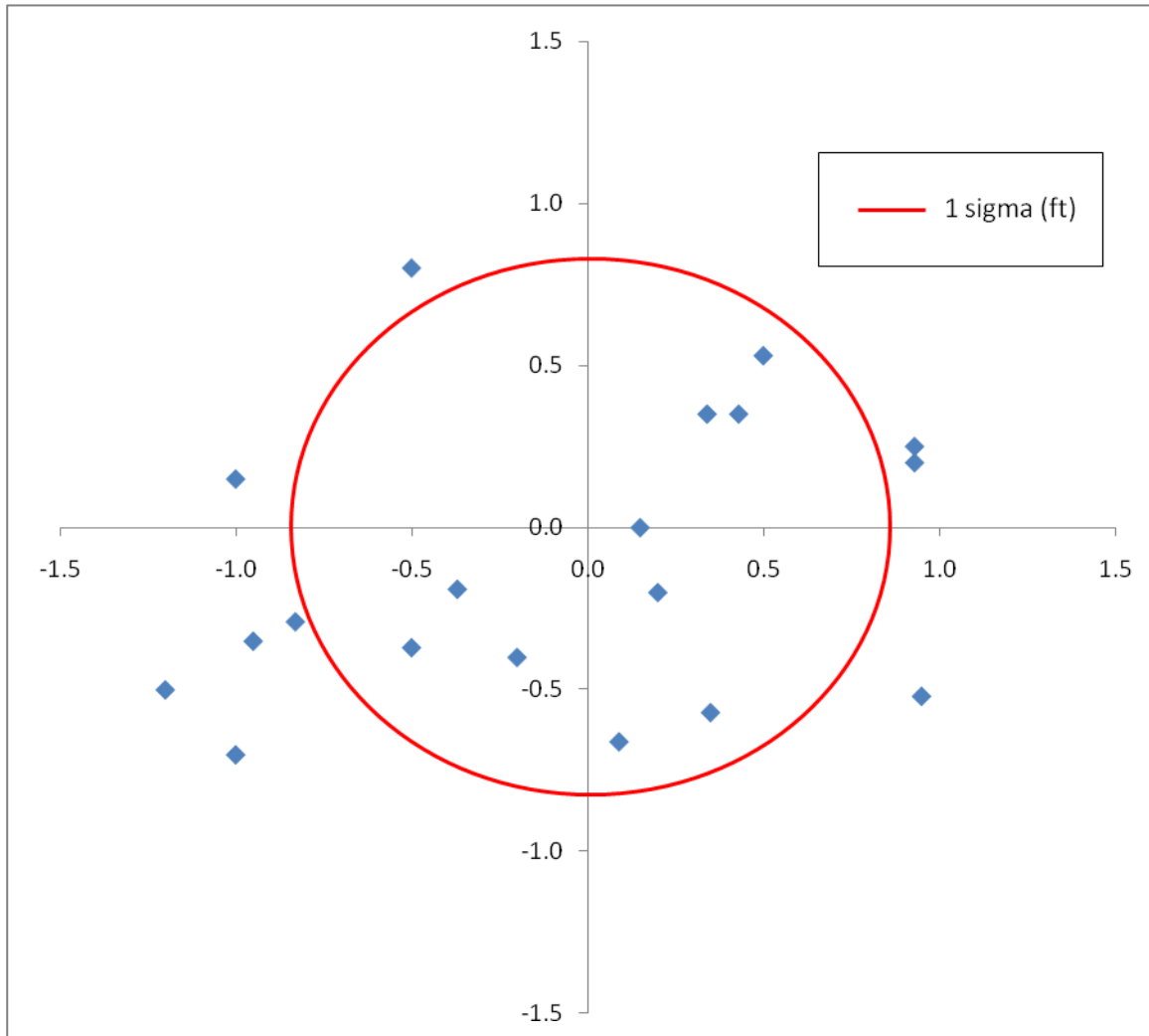


Aerial imagery accuracies for the Cottonwood Canyon study area are found in **Figure 9**, **Figure 10** and **Table 4** below.

Table 4. Deviation between aerial photos and intensity images based on 20 accuracy check points

	Mean	Standard Deviation (1 Sigma)	Root Mean Square Error (RMSE)
Cottonwood Canyon Photos	0.14 ft	0.83 ft	0.82 ft

Figure 10. Checkpoint residuals derived from comparing aerial photos to intensity images; deviations are in feet.



7. Projection/Datum and Units

Projection:		Oregon Lambert, International Feet
Datum	Vertical:	NAVD88 Geoid03
	Horizontal:	NAD 83 (CORS 96)
Units:		Feet

8. Deliverables

Point Data:	<ul style="list-style-type: none"> • All laser returns (LAS v. 1.2 format) • Ground classified returns (LAS v. 1.2 format)
Vector Data:	<ul style="list-style-type: none"> • Study area boundary (shapefile format) • SBETs (shape file format) • LiDAR/Ortho Photo/Intensity 0.75' quadrangle delineation (shapefile format) • DEM 3.75' quadrangle delineation (shapefile format)
Raster Data:	<ul style="list-style-type: none"> • Elevation models (3 ft resolution): <ul style="list-style-type: none"> • Bare Earth Model (ESRI GRID format) • Highest Hit Model (ESRI GRID format) • Intensity images (GeoTIFF format; 1.5 ft resolution) • Ortho photo tiles (GeoTIFF format 15 cm resolution)
Data Report:	<ul style="list-style-type: none"> • Full report containing introduction, methodology, and accuracy

9. Selected Images

Figure 11. Orthophotograph referenced to highest hit model looking northwest along the Esau Canyon River.

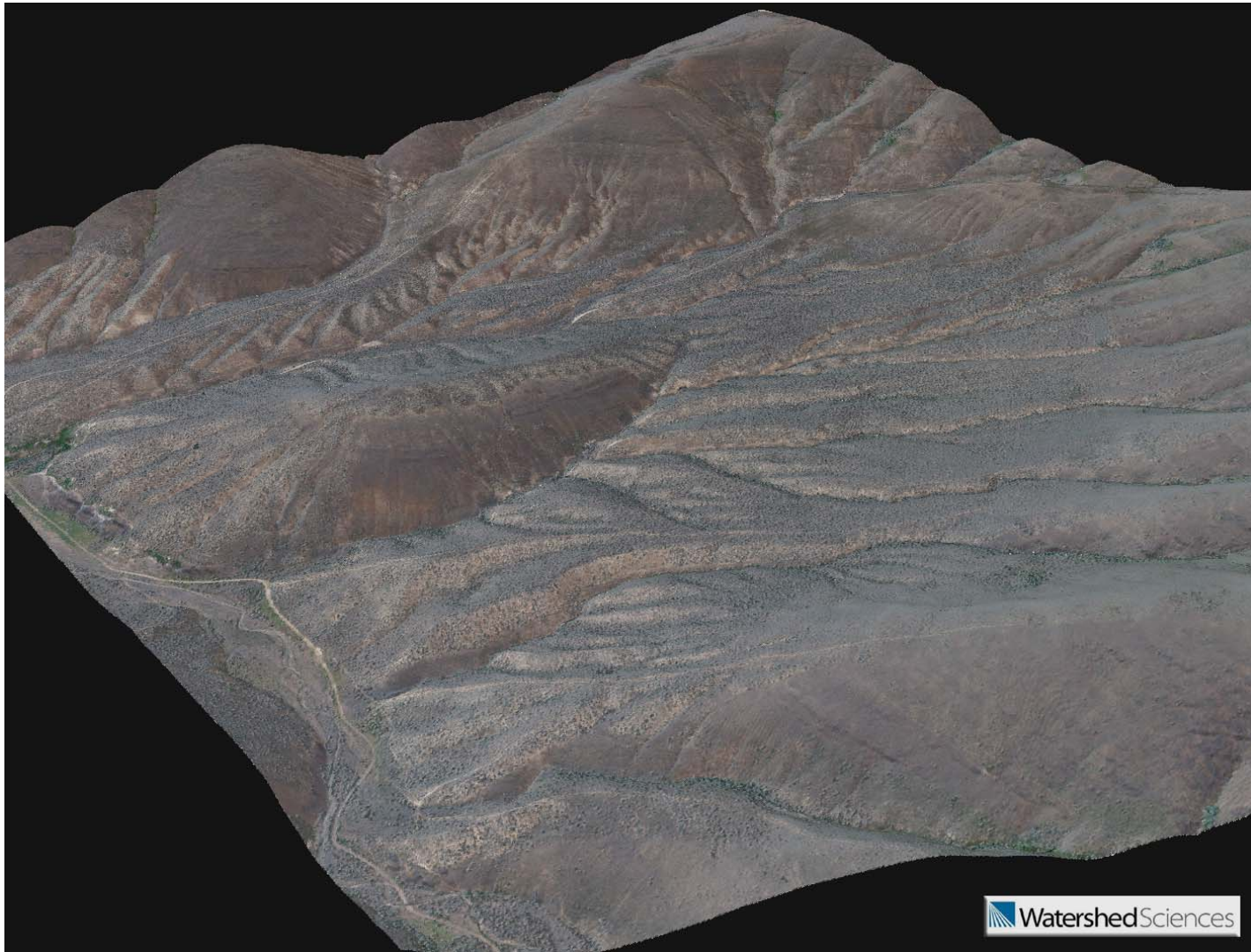


Figure 12. Orthophotograph referenced to highest hit model. View is looking north along the John Day River just west of route 206.



Figure 13. 3D LiDAR point cloud colored by orthophotograph RGB values, the view is along the John Day River.



Figure 14. Orthophotograph referenced to highest hit model looking west with the John Day River in the foreground just south of JS Burres State Park.



10. Glossary

1-sigma (σ) Absolute Deviation: Value for which the data are within one standard deviation (approximately 68th percentile) of a normally distributed data set.

2-sigma (σ) Absolute Deviation: Value for which the data are within two standard deviations (approximately 95th percentile) of a normally distributed data set.

Root Mean Square Error (RMSE): A statistic used to approximate the difference between real-world points and the LiDAR points. It is calculated by squaring all the values, then taking the average of the squares and taking the square root of the average.

Pulse Rate (PR): The rate at which laser pulses are emitted from the sensor; typically measured as thousands of pulses per second (kHz).

Pulse Returns: For every laser pulse emitted, the Leica ALS 50 Phase II system can record *up to four* wave forms reflected back to the sensor. Portions of the wave form that return earliest are the highest element in multi-tiered surfaces such as vegetation. Portions of the wave form that return last are the lowest element in multi-tiered surfaces.

Accuracy: The statistical comparison between known (surveyed) points and laser points.

Typically measured as the standard deviation (σ) and root mean square error (RMSE).

Intensity Values: The peak power ratio of the laser return to the emitted laser. It is a function of surface reflectivity.

Data Density: A common measure of LiDAR resolution, measured as points per square meter.

Spot Spacing: Also a measure of LiDAR resolution, measured as the average distance between laser points.

Nadir: A single point or locus of points on the surface of the earth directly below a sensor as it progresses along its flight line.

Scan Angle: The angle from nadir to the edge of the scan, measured in degrees. Laser point accuracy typically decreases as scan angles increase.

Overlap: The area shared between flight lines, typically measured in percents; 100% overlap is essential to ensure complete coverage and reduce laser shadows.

DTM / DEM: These often-interchanged terms refer to models made from laser points. The digital elevation model (DEM) refers to all surfaces, including bare ground and vegetation, while the digital terrain model (DTM) refers only to those points classified as ground.

Real-Time Kinematic (RTK) Survey: GPS surveying is conducted with a GPS base station deployed over a known monument with a radio connection to a GPS rover. Both the base station and rover receive differential GPS data and the baseline correction is solved between the two. This type of ground survey is accurate to 1.5 cm or less.

11. Citations

Soininen, A. 2004. TerraScan User's Guide. TerraSolid.

Appendix A

LiDAR accuracy error sources and solutions:

Type of Error	Source	Post Processing Solution
GPS (Static/Kinematic)	Long Base Lines	None
	Poor Satellite Constellation	None
	Poor Antenna Visibility	Reduce Visibility Mask
Relative Accuracy	Poor System Calibration	Recalibrate IMU and sensor offsets/settings
	Inaccurate System	None
Laser Noise	Poor Laser Timing	None
	Poor Laser Reception	None
	Poor Laser Power	None
	Irregular Laser Shape	None

Operational measures taken to improve relative accuracy:

Low Flight Altitude: Terrain following is employed to maintain a constant above ground level (AGL). Laser horizontal errors are a function of flight altitude above ground (i.e., $\sim 1/3000^{\text{th}}$ AGL flight altitude).

Focus Laser Power at narrow beam footprint: A laser return must be received by the system above a power threshold to accurately record a measurement. The strength of the laser return is a function of laser emission power, laser footprint, flight altitude and the reflectivity of the target. While surface reflectivity cannot be controlled, laser power can be increased and low flight altitudes can be maintained.

Reduced Scan Angle: Edge-of-scan data can become inaccurate. The scan angle was reduced to a maximum of $\pm 14^\circ$ from nadir, creating a narrow swath width and greatly reducing laser shadows from trees and buildings.

Quality GPS: Flights took place during optimal GPS conditions (e.g., 6 or more satellites and PDOP [Position Dilution of Precision] less than 3.0). Before each flight, the PDOP was determined for the survey day. During all flight times, a dual frequency DGPS base station recording at 1-second epochs was utilized and a maximum baseline length between the aircraft and the control points was less than 19 km (11.5 miles) at all times.

Ground Survey: Ground survey point accuracy (i.e. < 1.5 cm RMSE) occurs during optimal PDOP ranges and targets a minimal baseline distance of 4 miles between GPS rover and base. Robust statistics are, in part, a function of sample size (n) and distribution. Ground survey RTK points are distributed to the extent possible throughout multiple flight lines and across the survey area.

50% Side-Lap (100% Overlap): Overlapping areas are optimized for relative accuracy testing. Laser shadowing is minimized to help increase target acquisition from multiple scan angles. Ideally, with a 50% side-lap, the most nadir portion of one flight line coincides with the edge (least nadir) portion of overlapping flight lines. A minimum of 50% side-lap with terrain-followed acquisition prevents data gaps.

Opposing Flight Lines: All overlapping flight lines are opposing. Pitch, roll and heading errors are amplified by a factor of two relative to the adjacent flight line(s), making misalignments easier to detect and resolve.

Appendix B

1 Cottonwood Canyon Mapping Control Report July 23, 2010

This report describes efforts to establish mapping control for the Cottonwood Canyon LiDAR project. Two mapping control monuments were established using global positioning system (GPS) receivers. The mapping control monuments provide a recoverable location upon which differential corrections can be generated by the GPS receivers. The differential corrections are used to adjust measurements collected by a GPS receiver on board the LiDAR aircraft and for a GPS roving receiver collecting real time kinematic (RTK) data. These monuments are not intended to serve any other purpose.

A. Monument name and number

Two monuments were established:

1. CC-AW1
2. CC-AW2

B. Monument location: Section, Township, and Range

1. CC-AW1: S9 T2S R19E
2. CC-AW2: S9 T2S R19E

C. Horizontal coordinates

CC-AW1

Northing (Y) [meters] 193223.988 State plane coordinate (3601 OR N)

Easting (X) [meters] 2504384.679 State plane coordinate (3601 OR N)

Convergence [degrees] 0.03972291

Point Scale 0.99990310

Combined Factor 0.99980545

Latitude (ellipsoidal) 45° 24' 19.79846''

Longitude (ellipsoidal) 120° 26' 38.35690''

Datum NAD_83(CORS96)

CC-AW2

Northing (Y) [meters] 194197.844 State plane coordinate (3601 OR N)

Easting (X) [meters] 2503832.284 State plane coordinate (3601 OR N)

Convergence [degrees] 0.03472384

Point Scale 0.99990375

Combined Factor 0.99980982

Latitude (ellipsoidal) 45° 24' 51.35794''

Longitude (ellipsoidal) 120° 27' 3.73336''

Datum NAD_83(CORS96)

D. Vertical coordinates

CC-AW1

Ellipsoidal (GRS80 (m)): 623.000

Orthometric (Geod03 (m)): 644.171

Geoid Separation (m): -21.171

CC-AW2

Ellipsoidal (GRS80 (m)): 599.202

Orthometric (Geod03 (m)): 620.403

Geoid Separation (m): - 21.201 2

E. Date of survey

Initial GPS observations were collected on May 13-15, 2010. Final processing of the GPS observations occurred on July 20, 2010.

F. Business name and address of surveyor

Watershed Sciences, Inc.

517 SW 2nd St. Suite 400

Corvallis, OR 97333

Michael Wing, PLS

G. Monument description and location narrative

CC-AW1:

From Condon, OR head W/NW on OR Hwy 206 and continue 20 miles to monument on left (W) side of road. Monument is located 15' W from edge of road, and 6' E of fence-line. Monument is a 2" aluminum cap stamped "Watershed Sciences, Inc" around the outside, and "2010 CC-AW1" in the middle. Monument cap is placed on a 5/8" by 30" rebar.

CC-AW2:

From Condon, OR head W/NW on OR Hwy 206 and continue 20.8 miles to monument on left (W) side of road at the top of a sloping embankment. Monument is located 75' W of edge of road, and 8' E of fence-line. Monument is a 2" aluminum cap stamped "Watershed Sciences, Inc" around the outside, and "2010 CC-AW2" in the middle. Monument is placed on a 5/8" by 30" rebar.

H. Purpose of the survey, equipment and procedures used, geoid model and reference ellipsoid used.

The purpose of the Cottonwood Canyon Mapping Control project was to establish two mapping control monuments in support of measurements collected during a LiDAR data acquisition project. Two mapping control monuments were established using global positioning system (GPS) receivers. The mapping control monuments provide a recoverable location upon which differential corrections can be generated by the GPS receivers. The differential corrections are used to adjust measurements collected by a GPS receiver on board the LiDAR aircraft and

for a GPS roving receiver collecting real time kinematic (RTK) data. These monuments are not intended to serve any other purpose.

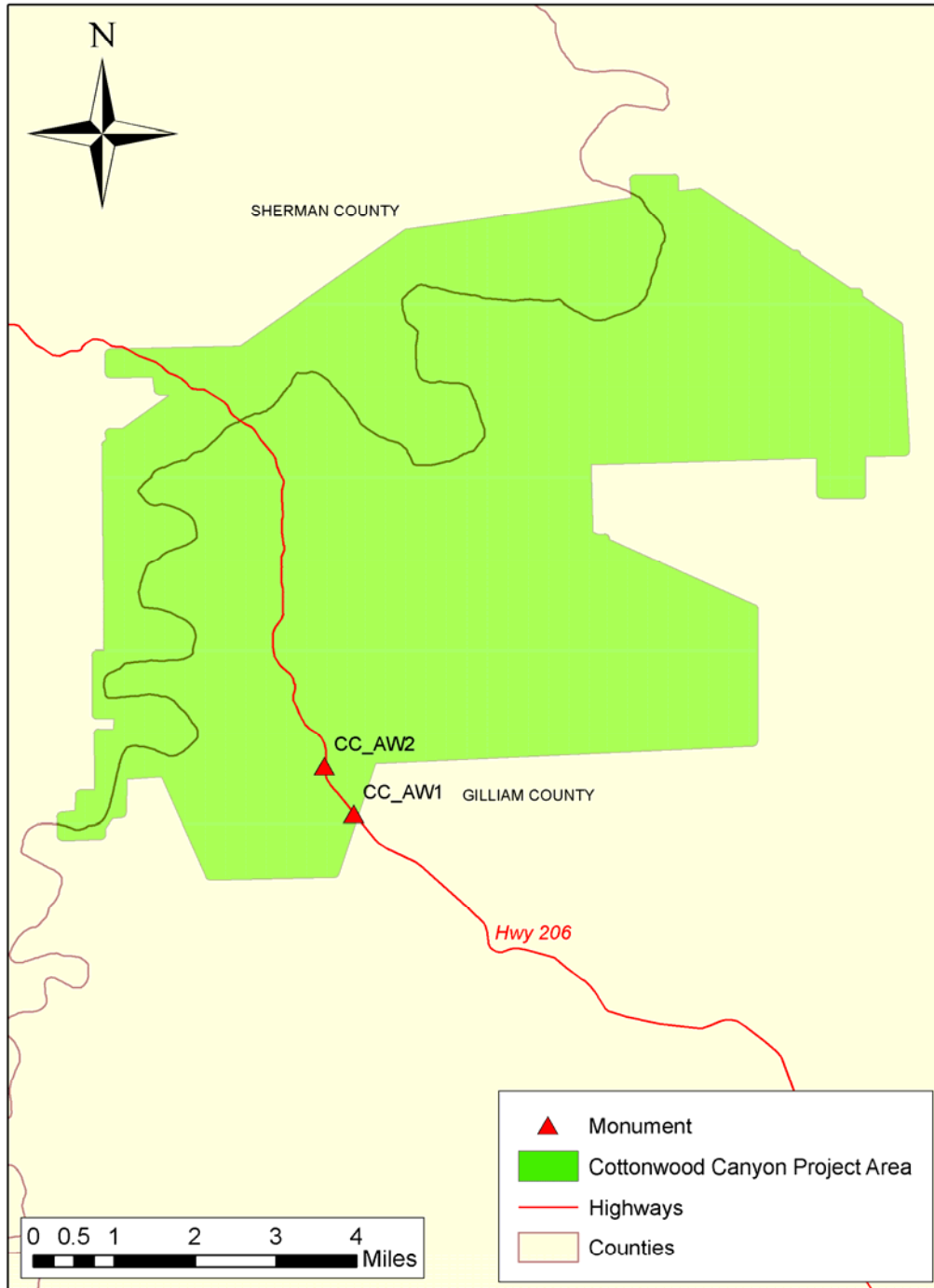
GPS observations were collected on both monuments (CC-AW1 and CC-AW2) during three time periods. The initial observation time occurred on May 13, 2010 during the LiDAR flight and spanned over seven (7) hours on both monuments. Subsequent GPS observations also occurred on May 14 and May 15 with different antenna reference points (ARPs). The subsequent observations were used to confirm the measurement consistency of the initial observations.

Geoid and reference ellipsoid are described in section D of this report.

Both monuments were occupied by Trimble R7 GNSS receivers with Zephyr Geodetic antennas. GPS measurements were processed using the National Geodetic Survey (NGS) Online Positioning User Service (OPUS). OPUS provides differentially corrected coordinates based on an average calculated from three independent single-baseline solutions from surrounding Continuously Operating Reference Stations (CORS).

I. Map

Cottonwood Canyon Mapping Control



This map is intended to show the relative locations of two mapping control monuments in relation to surrounding landscape features. No guarantee or assurance is intended or provided as to the positional accuracy of any feature or object shown on this map.

J. Seal and signature



K. Network and local accuracy

The following results are drawn directly from the OPUS solution output.

CC-AW1

Horizontal network accuracy 0.00272(m)

Vertical network accuracy 0.00239(m)

CC-AW1 Peak-to-peak errors

Latitude (ellipsoidal) 0.022(m)

Longitude (ellipsoidal) 0.021(m)

Ellipsoidal height 0.023(m)

Orthometric height 0.023(m)

CC-AW2

Horizontal network accuracy 0.00347(m)

Vertical network accuracy 0.00302(m)

CC-AW2 Peak-to-peak errors

Latitude (ellipsoidal) 0.039(m)

Longitude (ellipsoidal) 0.032(m)

Ellipsoidal height 0.003(m)

Orthometric height 0.003(m)